City Research Online

City, University of London Institutional Repository

Article

Two-Dimensional vs. Three-Dimensional FE Modeling of Skin and Proximity Effects in Segmented Cables with Parallel Conductors: A Comparative Study

Soheil Ahmadi *[iD]**, S. H. Khan and K. T. V. Grattan**

Engineering Department, City St George's, University of London, London EC1V 0HB, UK;
s.h.khan@citystgeorges.ac.uk (S.H.K.); k.t.v.grattan@citystgeorges.ac.uk (K.T.V.G.)
* Correspondence: soheil.ahmadi@citystgeorges.ac.uk (S.A.)

Abstract: This paper investigates the influence of skin and proximity effects on power losses in segmented power cables using finite element (FE) analysis. Two-dimensional (2D) and three-dimensional (3D) FE models are developed to evaluate the AC-to-DC resistance ratio (R_{AC}/R_{DC}) in single-, three-, and five-segment cable configurations. Frequencies of 0, 50, 150, and 250 Hz are considered under an infinite lay length (parallel strands) assumption. This study reveals that 2D modeling provides nearly identical R_{AC}/R_{DC} values to 3D, with deviations of less than 0.6% at 50 Hz when no twisting is present. This highlights the computational efficiency of 2D models for certain cable designs without compromising accuracy. Furthermore, this paper examines the mesh refinement and sub-conductor geometry (hexagonal packing) of underground cables under full compression assumption. The results underscore the viability of 2D cross-sectional simulations for multi-segment cables, ensuring accurate loss predictions while saving considerable computational resources.

Keywords: AC losses; eddy current; electromagnetic analysis; proximity effect; skin effect

1. Introduction

High-voltage power cables often exhibit significant skin and proximity effects when carrying alternating current (AC). The skin effect concentrates current near the conductor surface, effectively reducing the cross-sectional area for current flow and thus raising the AC resistance [1]. The proximity effect further distorts current distribution in the presence of neighboring conductors, potentially increasing losses [2]. These effects become especially pronounced in large-diameter conductors and at elevated frequencies [3].

To mitigate AC losses, segmented cables (Milliken designs) are subdivided into multiple lobes or bundles, often separated by thin insulation or air gaps [4,5]. Accurate simulation of such designs typically involves finite element (FE) methods, which are flexible enough to capture complex geometries [6].

However, 3D finite-element analysis is computationally expensive, especially for cables with hundreds of strands [7]. Under certain conditions—most notably, an infinite lay length or purely parallel conductor strands—2D cross-sectional simulations can approximate 3D results well. Various studies [8] confirm that when no helical twist is present, 2D and 3D solutions for skin and proximity losses vary only a few percent.

All conductors in this study are considered to have a hexagonal cross-section, as this shape is typical under full compression [9]. This design minimizes voids and optimizes packing efficiency in cables, ensuring reduced AC resistance. Figure 1 illustrates the difference between uncompressed and fully compressed cross-sectional configurations.

Hexagonal segments are particularly relevant for evaluating skin and proximity effects due to their uniformity and predictability.
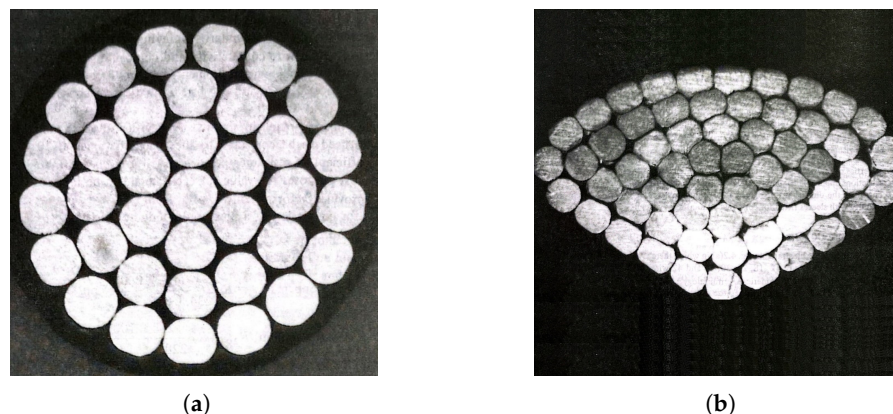

(**a**)	(**b**)

Figure 1. Cross-sectional views of uncompressed (**a**) and compressed (**b**) multi-segment cables [9].

High-voltage power cables often carry currents with a dominant fundamental frequency of 50 Hz [10]. However, higher-order harmonics, particularly the 3rd (150 Hz) and 5th (250 Hz) harmonics, frequently arise in power systems due to nonlinear loads and switching devices [11]. These harmonics contribute disproportionately to additional losses because their higher frequencies exacerbate the skin and proximity effects. Hence, the 3rd and 5th harmonics are also selected for simulation to capture their impact on R_{AC}/R_{DC}.

This paper systematically compares 2D vs. 3D FE for single-, three-, and five-segment cables under frequencies 0, 50, 150, and 250 Hz. We expand upon the earlier validation in [12], employing hexagonal sub-conductors to simulate full compression. The principal questions are as follows:

- How accurately does 2D match 3D for each model?
- How do additional segments affect R_{AC}/R_{DC} across various frequencies?
- What computational savings arise from 2D modeling?

Results indicate that 2D runs provide accurate predictions (<2% deviation) at all tested frequencies for parallel-lay cables.

2. Skin and Proximity Effect Losses

2.1. Skin and Proximity Effect

The phenomenon where alternating current tends to flow more intensely near the surface of a conductor is known as the *Skin Effect*. This effect is caused by eddy currents generated as a result of a changing magnetic field [13]. In the presence of neighboring conductors carrying AC, their changing magnetic fields further distort the current distribution, leading to the *Proximity Effect* [14].

2.2. Definition of the R_{DC} and the P_{2D}

Considering a long homogeneous conductor carrying direct current (DC), the current is uniformly distributed across the conductor [15]. The total resistance of the wire can be calculated using

$$R_{DC} = \frac{\rho l}{S} \quad (\Omega), \tag{1}$$

where S is the cross-sectional area, l is the length, and ρ is the resistivity of the material [16]. The unit is Ohms (Ω).

For a 2D model, as shown in Figure 2a, the circular cross-section of the wire is divided into a finite number of filaments. The resistance per unit length (Ω/m) is given as

$$R_{\text{DC-2D}} = \frac{\rho}{S} \quad (\Omega/\text{m}). \tag{2}$$
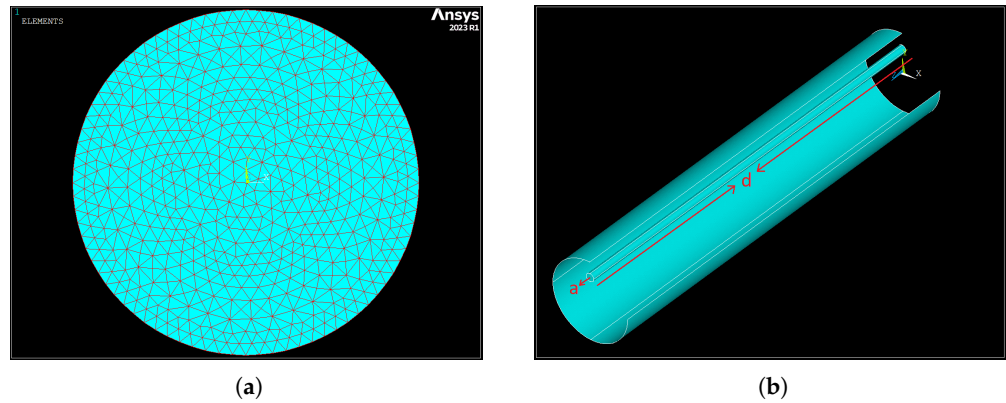

(**a**) (**b**)

Figure 2. A solid round wire divided into a finite number of filaments in 2D (**a**). A filament within a solid round wire in 3D with section area a and length d (**b**).

The total power dissipated by the conductor can then be expressed as

$$P = I^2 R_{\text{DC}} \quad (\text{W}), \tag{3}$$

where P is the total dissipated power in Watts (W), I is the current in Amps (A), and R_{DC} is the DC resistance in Ohms (Ω).

For 2D analysis, the power loss per unit length is:

$$P_{2D} = I^2 R_{\text{DC-2D}} \quad (\text{W/m}). \tag{4}$$

2.3. Definition of the R_{AC}

When the wire is divided into multiple filaments, each filament has a section area a, length d, and electrical conductivity σ. Figure 2b visualises a filament within the entire wire in three-dimension. For a single filament, the resistance can be calculated as

$$R_{\text{f}} = \frac{d}{\sigma a} \quad (\Omega), \tag{5}$$

and in 2D analysis

$$R_{\text{f-2D}} = \frac{1}{\sigma a} \quad (\Omega/\text{m}). \tag{6}$$

For uneven current distribution in the 2D conductor (Figure 2a) caused by an alternative current, each filament has a unique current density J_f (A/m^2) and resistance $R_{\text{f-2D}}$. The power dissipated in each filament is

$$P_{f\text{-2D}} = J_f^2 R_{\text{f-2D}} = J_f^2 \frac{1}{\sigma a} \quad (\text{W/m}). \tag{7}$$

The total power loss per unit length in the conductor in 2D is obtained by integrating over the total section area S:

$$P_{2D} = \int_S P_{f\text{-2D}} \, \text{d}s \quad (\text{W/m}). \tag{8}$$

In transitioning to the continuous framework, the discrete filament cross-sectional area a becomes unnecessary because the integral assumes a continuous distribution, reflecting the shift from summation to integration over the conductor's cross-sectional area. The term $\text{d}s$ inherently represents the infinitesimal contribution of the area. Thus,

$$P_{2D} = \int_S J^2 \frac{1}{\sigma} \, ds \quad (\text{W/m}), \tag{9}$$

the total AC resistance of the wire in 2D is then defined as

$$R_{AC} = \frac{\int_S J^2 \frac{1}{\sigma} \, ds}{I^2} \quad (\Omega/\text{m}). \tag{10}$$

2.4. Definition of the R_{AC}/R_{DC} Ratio

The ratio R_{AC}/R_{DC} can be calculated by dividing both sides of (10) by the DC resistance:

$$\frac{R_{AC}}{R_{DC}} = \frac{\int_S J^2 \frac{1}{\sigma} \, ds}{I^2 R_{DC}}. \tag{11}$$

This ratio removes the dependency on variable parameters from different models, enabling straightforward comparisons.

2.5. Definition of the Skin Depth

The skin depth (δ) is a critical parameter for analyzing skin effect losses in conductors. It quantifies the depth below the conductor surface at which the current density decreases to approximately 37% of its value at the surface. In another word, (δ) is the depth at which the current density decays to $1/e$ of its surface value. Figure 3 illustrates the exponential decay of current density within a conductor. The skin depth is given by [13]

$$\delta = \sqrt{\frac{2}{\omega \mu \sigma}}, \tag{12}$$

where

- $\omega = 2\pi f$ is the angular frequency (rad/s);
- μ is the magnetic permeability (H/m);
- σ is the electrical conductivity (S/m).
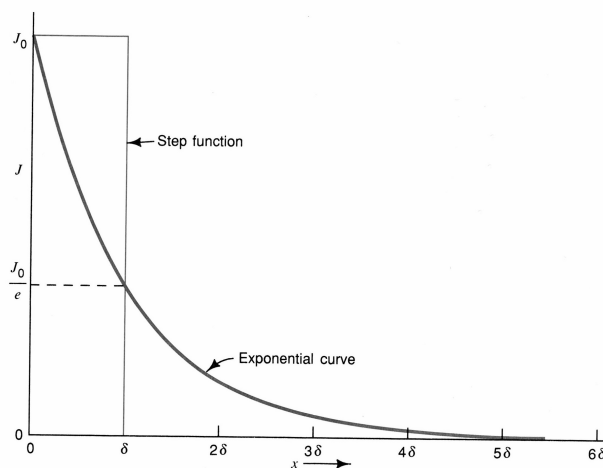

Figure 3. Current density versus distance from the surface of an AC-carrying conductor [15].

For copper, with $\sigma \approx 5.8 \times 10^7$ S/m and $\mu \approx \mu_0 = 4\pi \times 10^{-7}$ H/m, the skin depth at 50 Hz can be approximately calculated by using (12):

$$\delta = \sqrt{\frac{2}{2\pi(50)(4\pi \times 10^{-7})(5.8 \times 10^7)}} \approx 9.3 \, \text{mm}. \tag{13}$$

This indicates that at 50 Hz, the current is primarily confined to a thin outer layer of the conductor, and as the frequency increases, the skin depth decreases, intensifying the skin effect. This area is shown by the green circles on the 2D schematics in Figure 4.
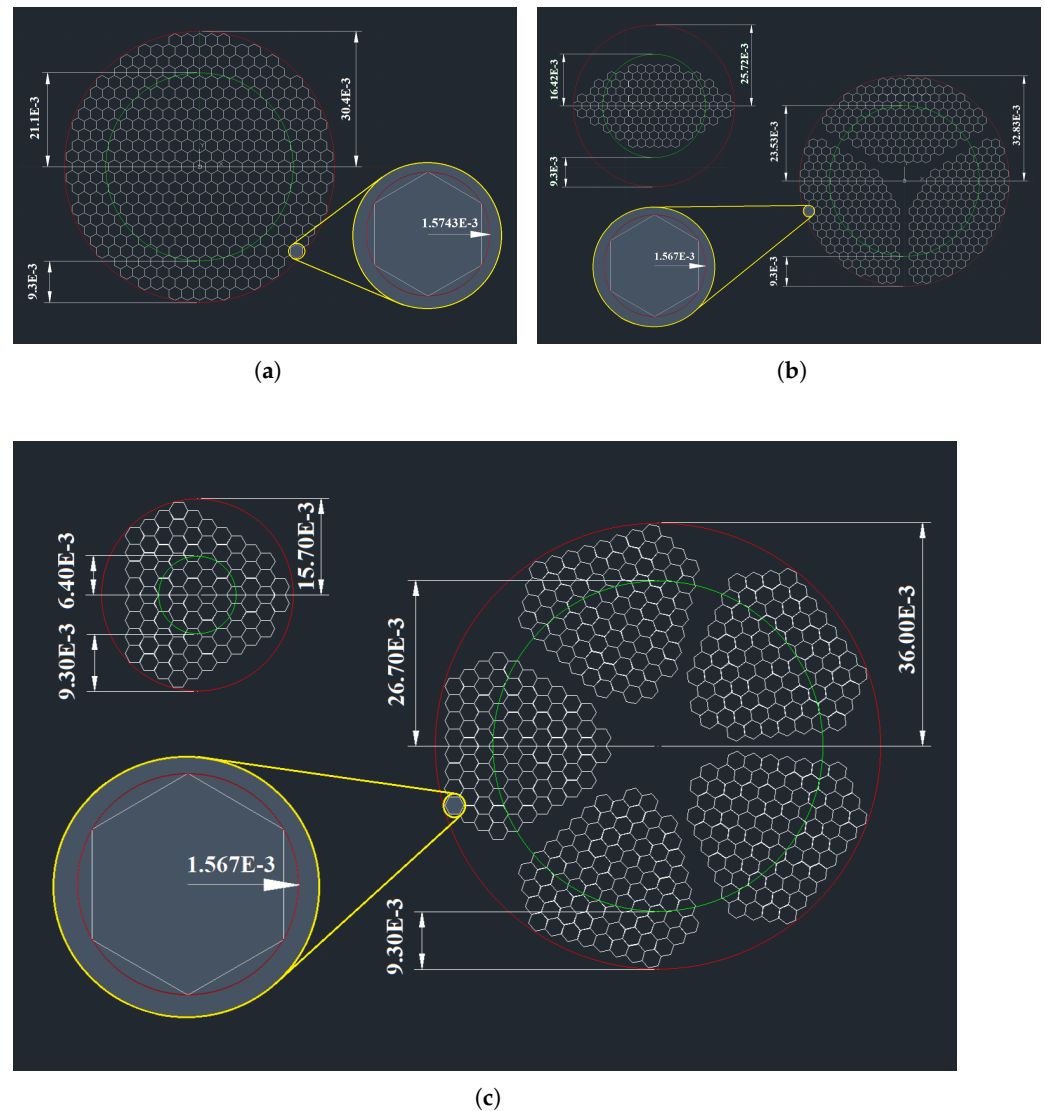

(**a**)   (**b**)

(**c**)

Figure 4. 2D segmented cable schematics for Single-segment (**a**), Three-segment (**b**) and Five-segment (**c**) arrangements; with all values in meter.

3. Cable Models and Methodology

This study compares three cable designs—single-segment, three-segment, and five-segment—under four operating frequencies (0, 50, 150, and 250 Hz). All simulations assume an infinite lay length (i.e., no helical twisting) to isolate the influence of conductor segmentation on electromagnetic losses. A consistent total conductor cross-sectional area of approximately 2711 mm^2 is maintained for each design, ensuring that differences in AC losses reflect segmentation rather than size.

3.1. Consistent Cross-Sectional Area and Segmentation

- Single-Segment (2D): The cable cross-section is one contiguous metallic cluster with about 421 hexagonal conductor strings. Each hex is sized so that the total copper area remains near 2711 mm^2. Figure 4a shows the layout for the single-segment 2D model;

- Three-Segment (2D): The same total area is subdivided into three segments, each separated by a small air gap. Approximately 143 hexagons per segment (total 429). Figure 4b illustrates this three-segment cross-section;
- Five-Segment (2D): Further subdivision into five segments, each holding around 85 hexagons (total 425). All five segments are isolated by small gaps. Figure 4c depicts the five-segment cross-section.

3.2. Transition from 2D to 3D: Extruded Models

Each 2D cross-section is extruded along the *z*-axis to form a 3D cable:

- Single-Segment 3D and Three-Segment 3D: Extruded by **1 m** (Figure 5a,b);
- Five-Segment 3D: Extruded by **4 m** (Figure 5c).

This difference in extrusion length (1 m vs. 4 m) helps determine whether longer axial spans cause deviations from 2D results when all conductors remain strictly parallel (no twisting).

(**a**)
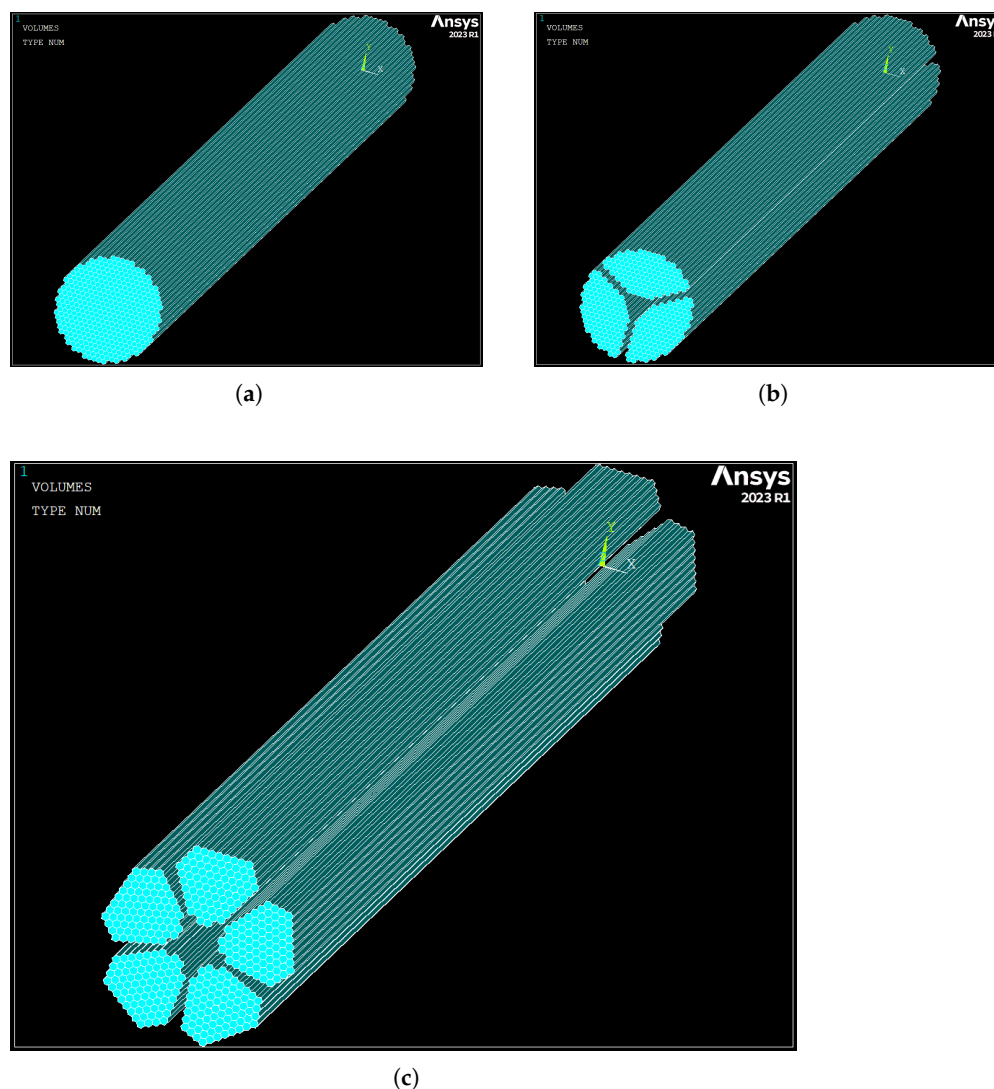(**b**)

(**c**)

Figure 5. Three-dimensional models of 1-segment (**a**), 3-segment (**b**), and 5-segment (**c**).

Although real cables often twist either the entire cross-section or each segment's conductors, these baseline 3D models omit such helical pitching. This isolates the effect of finite axial length alone before adding the complexity of twisting.

3.3. Material Properties and Air Boundary

Each cable model (whether 2D or 3D) is surrounded by a 30 cm thick layer of air in all radial directions, allowing the electromagnetic fields to decay naturally before reaching the simulation boundary. To approximate far-field conditions, the *magnetic vector potential* (*A*) is set to zero on the outer surface of this air region. This boundary condition prevents artificial reflection or confinement of the electromagnetic fields, thereby enhancing the realism of the results.

In harmonic (AC) analyses of power cables, only the relative permeability (μ_r) and electrical resistivity (ρ) of the conductor material (and air) are strictly required to capture frequency-dependent skin and proximity effects. Table 1 provides an overview of the material properties used in all simulations. Copper's high conductivity and air's near-zero conductivity ensure a clear distinction between conductor and non-conductive regions, facilitating accurate finite-element modeling of eddy currents and magnetic field distributions.

Table 1. Material properties used in simulations.

Material	μ_r	ρ ($\Omega \cdot$m)	σ (S/m)
Copper	1	1.7241×10^{-8}	5.8001×10^{7}
Air	1	1.0×10^{10}	1.0×10^{-10}

These properties remain fixed across all models for the frequencies tested (0–250 Hz).

3.4. Current Distribution and Frequencies

Analyses are performed at four frequencies: $0, 50, 150, 250$ Hz. A total of 10 A is applied to the coupled nodes of each cable cross-section area (2D) or the coupled nodes of one end of the extruded structure (3D). In multi-segment cables, this current is shared equally among segments (e.g., 3.33 A per segment for three segments) by coupling the voltage degree of freedome of each segment's nodes individually and applying the corresponding current portion to a node of each coupled set. By using an identical current input across all models, the comparisons of $R_{\text{AC}}/R_{\text{DC}}$ and AC loss factors remain consistent.

3.5. Verification and Reference

The geometry, solver configuration, and boundary conditions used here align with the finite-element approaches discussed in [12], ensuring numerical consistency and validating that the solver accurately captures skin and proximity effects under compressed conductor arrangements. Consequently, any observed difference between 2D and 3D results primarily reflects the effect of axial extrusion rather than inconsistencies in modeling assumptions.

4. Finite Element Setup

The finite element (FE) models in this study, developed using ANSYS Mechanical APDL 2023 R1 (developed by Ansys, Inc., Canonsburg, PA, USA), evaluate skin and proximity effect losses in multi-segment power cables. 2D models were run interactively on a standard PC (16 GB RAM, Intel® Core™ i5-8500 CPU), while more computationally intensive 3D models utilized high-performance computing (HPC) resources with up to 384 cores across eight machines (376 GB RAM per machine, 2 x "Intel® Xeon® Gold 6248R CPU @ 3.00 GHz" per machine) provided by City St George's University of London.

A *Solver Machine* framework—separately for 2D and 3D simulations—was implemented using APDL scripting. This framework standardized the simulation setup, including boundary conditions, meshing, and solver settings, across different geometric

configurations to ensure consistency. Iterative solvers were used to achieve reliable results with consistent simulation error.

Magnetic Edge Analysis was utilized, configured with the Harmonic Analysis, allowing detailed investigation of skin and proximity effects in cables. These advanced setups and methodologies ensured that the models provided robust and accurate representations of eddy-currents and steady-state current distribution in high-voltage power cables.

4.1. Two-Dimensional Modeling Approach

The 2D FE model captures the cross-sectional behavior of the cables under study. It is particularly suitable for configurations where all conductors are parallel, as the electromagnetic fields remain uniform along the longitudinal axis. Table 2 indicates the total number of elements for each 2D model. The key characteristics of these models are as follows:

- **Geometry:** The cross-section areas are modeled top-to-bottom, with length parameters specified to six decimal places, ensuring minimal modeling errors;
- **Element Type:** PLANE13 triangular elements with three nodes enabled coupled-field 2D electromagnetic analysis;
- **Material Allocation:** Table 1 properties were assigned to conductor and insulation elements;
- **Degrees of Freedom:** Voltage and magnetic vector potential (AZ) were coupled for electromagnetic continuity, with AZ grounded at the outmost layer to mimic the far-field;
- **Boundary Conditions:** The amplitude of the current excitation is applied to the conductor nodes as force;
- **Mesh Density:** A fine uniform mesh resolved the steady-state current density in conductors, while adaptive meshing (h-method) optimized accuracy and computational efficiency in air regions.

Table 2. Total number of elements and nodes for 2D models.

Model Configuration	Material	Elements	Nodes
1-Segment (2D)	Conductor	1,010,400	506,701
	Air	104,146	50,609
3-Segment (2D)	Conductor	1,029,600	517,743
	Air	286,028	140,108
5-Segment (2D)	Conductor	1,020,000	513,305
	Air	406,606	200,035

4.2. Three-Dimensional Modeling Approach

The 3D models accurately captures the longitudinal behavior of the cables under investigation. 2D geometries are initially exported as IGES (`.iges`) files and subsequently imported into the 3D simulation, ensuring consistent geometrical parameters. Table 3 shows the total number of elements for each 3D model with the following key characteristics:

- **Geometry:** The 2D geometry is extruded along the z-axis in untwisted configurations, ensuring the 3D models retain the same cross-sectional identities for accurate comparison;
- **Element Type:** SOLID237 tetrahedral elements enabled accurate coupled-field 3D electromagnetic analysis;
- **Material Allocation:** Similar to the 2D models, Table 1 properties are assigned to the 3D elements;

- **Degrees of Freedom:** Voltage and magnetic vector potential (AZ) were coupled for continuity, with AZ grounded at external nodes. Voltage was set to zero at one end of the cable's nodes to direct current flow;
- **Boundary Conditions:** Current exitation force is applied to the coupled nodes at the other end of the cable;
- **Mesh Density:** Fine and uniform meshes resolved current distribution in conductors, while adaptive meshing (h-method) optimized accuracy and efficiency in air regions.

Table 3. Total number of elements and nodes for 3D models.

Model Configuration	Material	Elements	Nodes
1-Segment (3D)	Conductor	1,109,053	1,581,938
	Air	468,059	518,748
3-Segment (3D)	Conductor	2,102,958	3,055,853
	Air	1,062,799	1,162,171
5-Segment (3D)	Conductor	5,265,862	7,958,575
	Air	4,107,837	4,509,268

4.3. FE Error

Discretization errors arise from approximating continuous electromagnetic fields using finite element meshes. These errors are influenced by mesh density and refinement, particularly in areas with steep field gradients, such as near conductors and insulation layers. Adaptive meshing helps reduce these errors by focusing on critical regions, improving accuracy without significantly increasing computational costs.To extract the maximum discretization error norms in ANSYS, the `EMAGERR` macro is typically used which provides error estimates for electromagnetic field quantities. The BN_{ERR} is the normalized measure of the discrepancy in the flux density (B) values presented in Table 4.

Table 4. Discretization errors for the FE models at 50 Hz.

Model	Region	2D-BN_{ERR} (%)	3D-BN_{ERR} (%)
1-Segment	Conductor	0.19	1.72
3-Segment	Conductor	0.22	1.24
5-Segment	Conductor	0.30	1.98

5. Results and Discussion

This section presents and critically analyzes the results obtained from both two-dimensional (2D) and three-dimensional (3D) finite element (FE) simulations of single-segment, three-segment, and five-segment cables. The primary focus is on comparing the AC-to-DC resistance ratio (R_{AC}/R_{DC}) across different segmentations and frequencies, assessing the accuracy of 2D models relative to their 3D counterparts, and evaluating the computational efficiency of each modeling approach. Additionally, the impact of segmentation and frequency on current distribution and magnetic field density is examined to provide comprehensive insights into the electromagnetic behavior of segmented cables.

5.1. R_{AC}/R_{DC} Ratio Comparison Between 2D and 3D Models

The R_{AC}/R_{DC} ratio serves as a critical metric for evaluating the influence of skin and proximity effects on power losses in segmented cables. Table 5 summarize the R_{AC}/R_{DC} ratios for both 2D and 3D models across single-segment, three-segment, and five-segment configurations at frequencies of 0 Hz, 50 Hz, 150 Hz, and 250 Hz.

Table 5. R_{AC}/R_{DC} ratios for 2D and 3D models.

Segment	Single-Segment		Three-Segment		Five-Segment	
Frequency (Hz)	2D	3D	2D	3D	2D	3D
0	1.00	1.00	1.00	1.00	1.00	1.00
50	1.85	1.86	1.76	1.76	1.74	1.75
150	3.04	3.07	2.91	2.92	2.88	2.91
250	3.88	3.93	3.70	3.74	3.66	3.72

Figure 6 graphically compares the R_{AC}/R_{DC} ratios obtained from 2D and 3D models across different segmentations and frequencies. The close alignment between 2D and 3D results across all configurations and frequencies underscores the efficacy of 2D modeling in accurately predicting AC losses without the computational burden associated with 3D simulations.
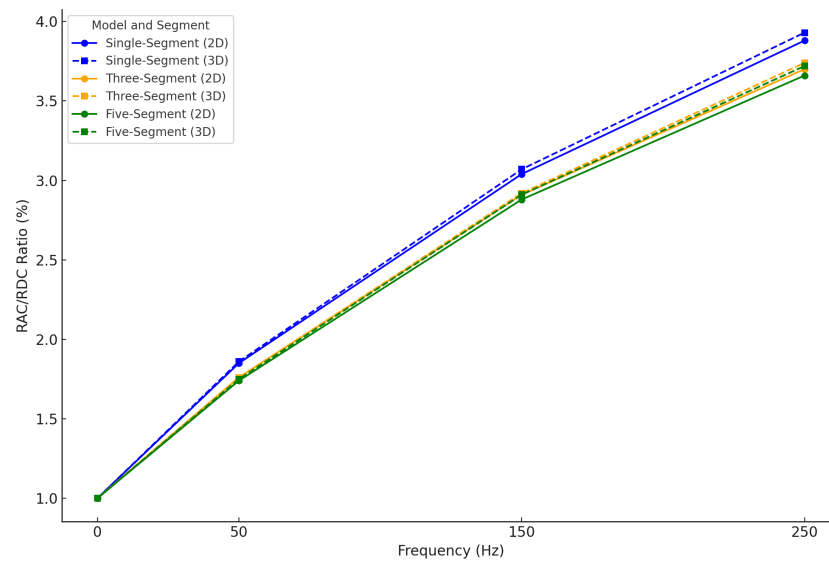

Figure 6. R_{AC}/R_{DC} ratios for 2D vs. 3D models across different segmentations and frequencies.

The marginal differences between 2D and 3D models, particularly at higher frequencies, are attributed to the increased complexity of accurately capturing electromagnetic phenomena in three dimensions. However, these discrepancies remain within an acceptable range (<2%), reinforcing the validity of using 2D models for certain cable designs without compromising accuracy.

5.2. Frequency Dependence of R_{AC}/R_{DC} Ratio

The R_{AC}/R_{DC} ratio exhibits a clear dependence on frequency, as expected due to the skin and proximity effects. Figure 6 illustrates the increase in the R_{AC}/R_{DC} ratio with frequency for single-segment, three-segment, and five-segment cables in both 2D and 3D models.

As frequency increases from 0 Hz to 250 Hz, the R_{AC}/R_{DC} ratio rises significantly across all segmentations. This trend is consistent with the theoretical understanding that higher frequencies lead to reduced skin depth (δ), confining more current to the conductor's surface and thereby increasing AC resistance. The rate of increase in the R_{AC}/R_{DC} ratio is consistent across different segmentations, indicating that while segmentation can mitigate the effects to some extent, the dominant influence is frequency-dependent.

5.3. Effect of Cable Segmentation on R_{AC}/R_{DC} Ratio

Segmentation plays a pivotal role in managing the skin and proximity effects within power cables. Figure 7 depicts the R_{AC}/R_{DC} ratios for single-segment, three-segment, and five-segment cables at 50 Hz.
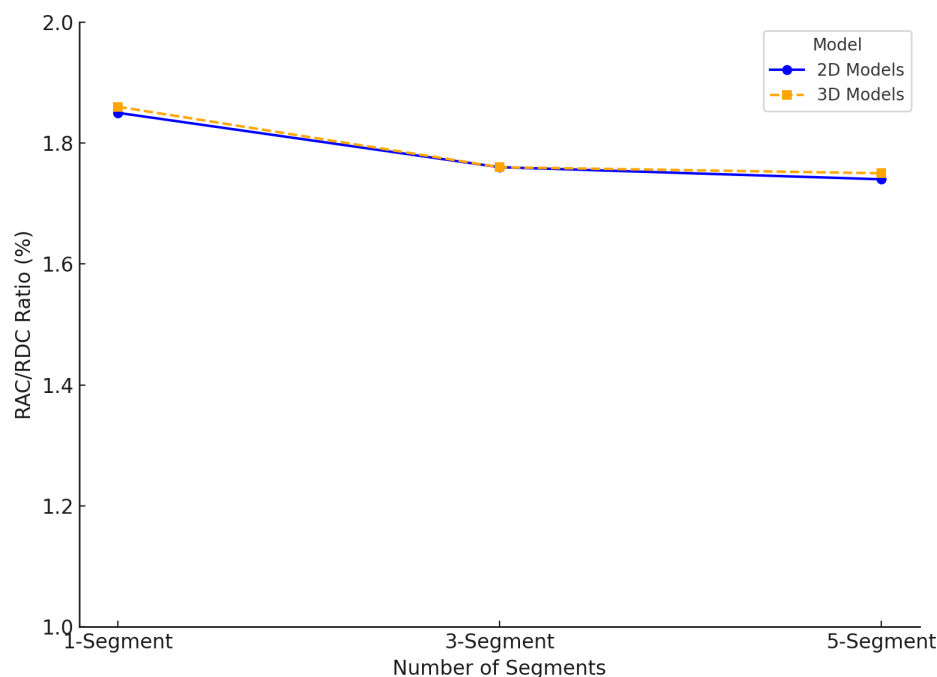

Figure 7. Impact of cable segmentation on R_{AC}/R_{DC} at 50 Hz.

The data reveal that increasing the number of segments from one to five results in a slight decrease in the R_{AC}/R_{DC} ratio. Specifically, at 50 Hz, the single-segment model exhibits a ratio of 1.85, which decreases to 1.74 in the five-segment model. This reduction suggests that segmentation distributes the current more evenly across the conductors, thereby mitigating the proximity effect and slightly reducing AC resistance. This presents a potential avenue for further study to explore innovative approaches for reducing skin and proximity effect losses.

5.4. Comparative Analysis Between 2D and 3D Models

A critical aspect of this study is the validation of 2D models against 3D models. Table 6 presents the relative percentage errors between the 2D and 3D models' R_{AC}/R_{DC} ratios across different segmentations and frequencies.

Table 6. Relative percentage error between 2D and 3D models.

Segment	50 Hz	150 Hz	250 Hz
Single-Segment	0.54%	0.99%	1.29%
Three-Segment	0.00%	0.34%	1.08%
Five-Segment	0.57%	1.04%	1.64%

These relative percentage errors are influenced by the discretization errors inherent in the FE models, as shown in Table 4. Notably, the five-segment 3D model, despite having a higher number of elements and nodes, exhibits a larger discretization error (2.39%) compared to the three-segment model (1.24%) due to its extended length of 4 m. Conversely, both the single-segment and three-segment 3D models are 1 m in length, but the three-

segment model benefits from a denser mesh structure, resulting in lower discretization errors. Key observations include the following:

- **Model Size and Segmentation:** The five-segment 3D model spans 4 m with 5,265,862 conductor elements and 7,958,575 nodes, leading to higher discretization errors. In contrast, the single and three-segment models are each 1 m long, with the three-segment model having a denser mesh (2,102,958 conductor elements and 3,055,853 nodes) compared to the single-segment model (1,109,053 conductor elements and 1,581,938 nodes), resulting in lower discretization errors.

- **Discretization Errors' Impact:** Higher discretization errors in 3D models, especially in larger and more segmented configurations, contribute to increased relative percentage errors between 2D and 3D models. For example, the five-segment model's higher discretization error (2.39%) aligns with its highest relative percentage error (1.64%) at 250 Hz.

- **Frequency Influence:** As frequency increases, skin and proximity effects become more pronounced, necessitating finer mesh resolutions. This requirement exacerbates discretization errors in 3D models, leading to higher relative percentage errors at elevated frequencies across all segmentations. Figure 8 visualizes the trend of increasing relative error with frequency across different segmentations.
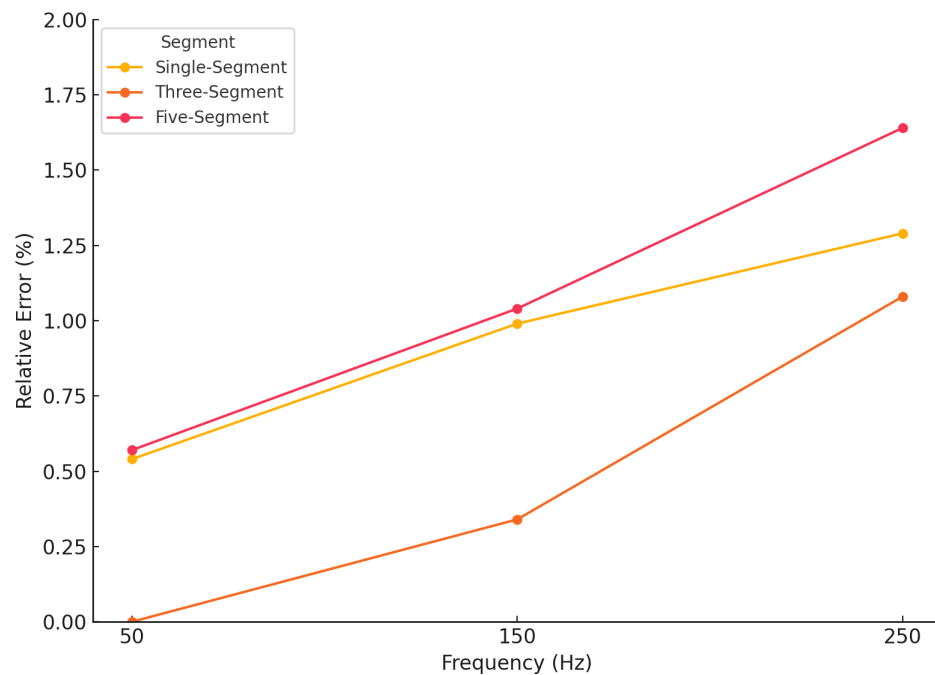

Figure 8. Percentage error between 2D and 3D models across frequencies for different segmentations.

5.5. Current Density Distribution Analysis

Current density distribution is pivotal in understanding the skin and proximity effects within conductors. This subsection presents both normalized current distribution line charts and color-coded current density maps for single-segment, three-segment, and five-segment 2D models at 50 Hz. These visualizations illustrate how segmentation and mesh density influence current distribution across the conductor's cross-section.

5.5.1. Color-Coded Current Density Maps

Figure 9a–c present color-coded maps of current density distribution for the 2D models, at 50 Hz. These maps use a color gradient from blue (lowest *J*) to red (highest *J*) to effectively illustrate the spatial distribution of current density across the conductor's cross-section. The

numerical values displayed on the color scale correspond to the range of current density (J) measured in amperes per square meter (A/m^2). The color-coded maps corroborate the findings from the line charts. The single-segment model shows a high concentration of red near the conductor's surface, highlighting the pronounced skin effect. The three-segment model exhibits a more uniform color distribution with fewer red regions, indicating a more balanced current flow due to its denser mesh. The five-segment model, while more segmented, still shows areas of high current density, particularly at the edges, which align with its higher discretization errors.
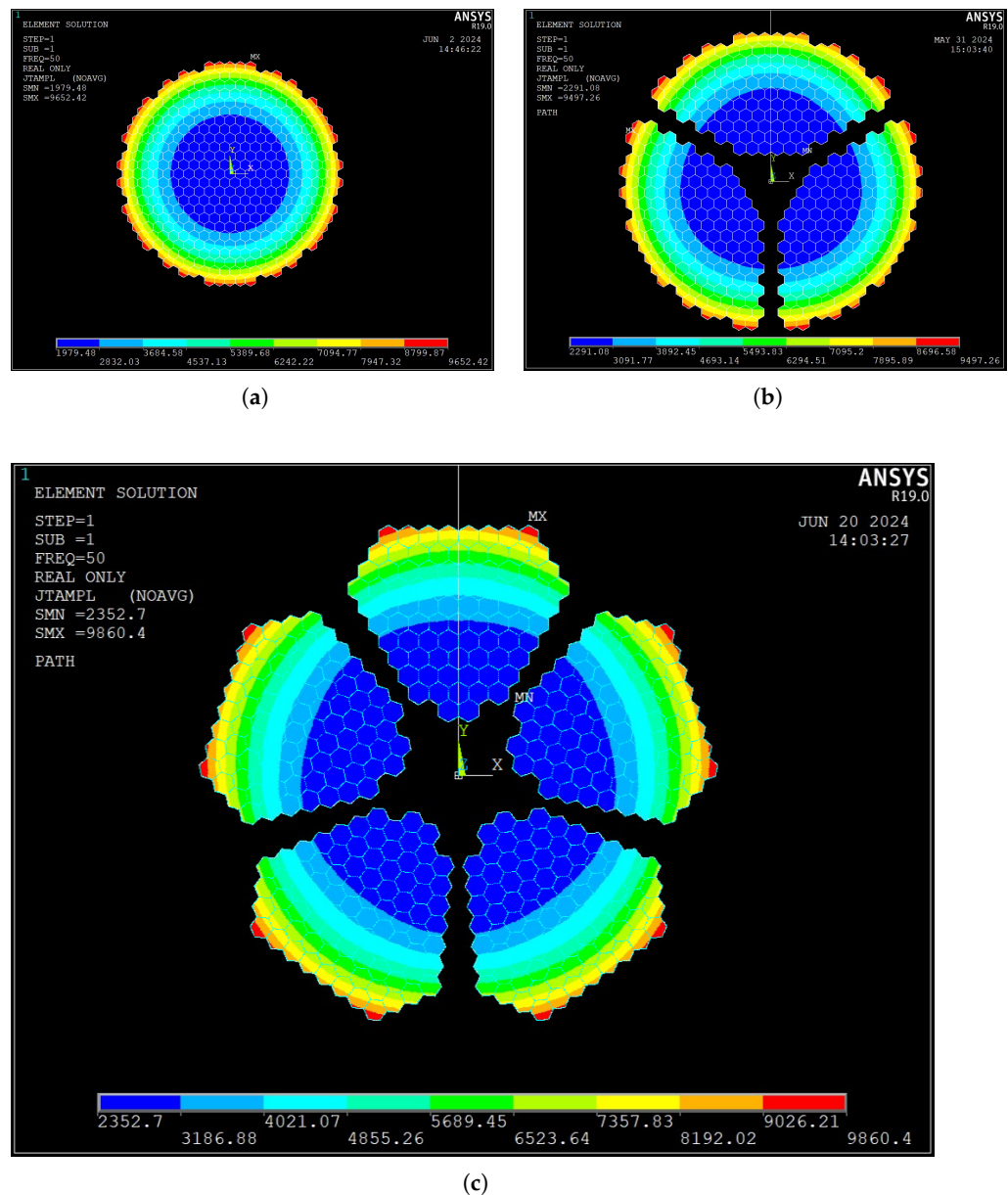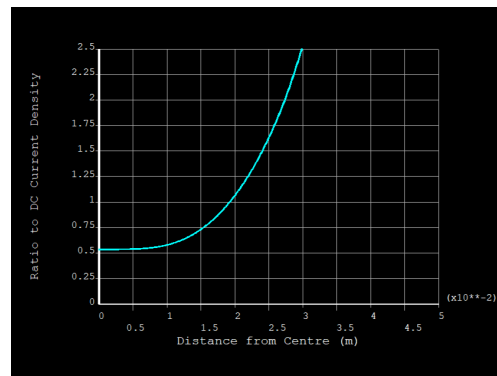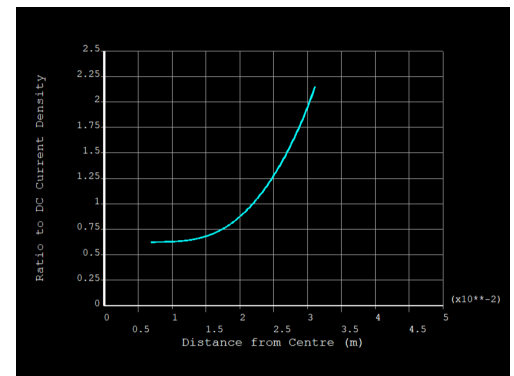

(**a**)

(**b**)

(**c**)

Figure 9. Current density distribution across conductor cross-section at 50 Hz (2D models) of 1-segment (**a**), 3-segment (**b**) and 5-segment (**c**).

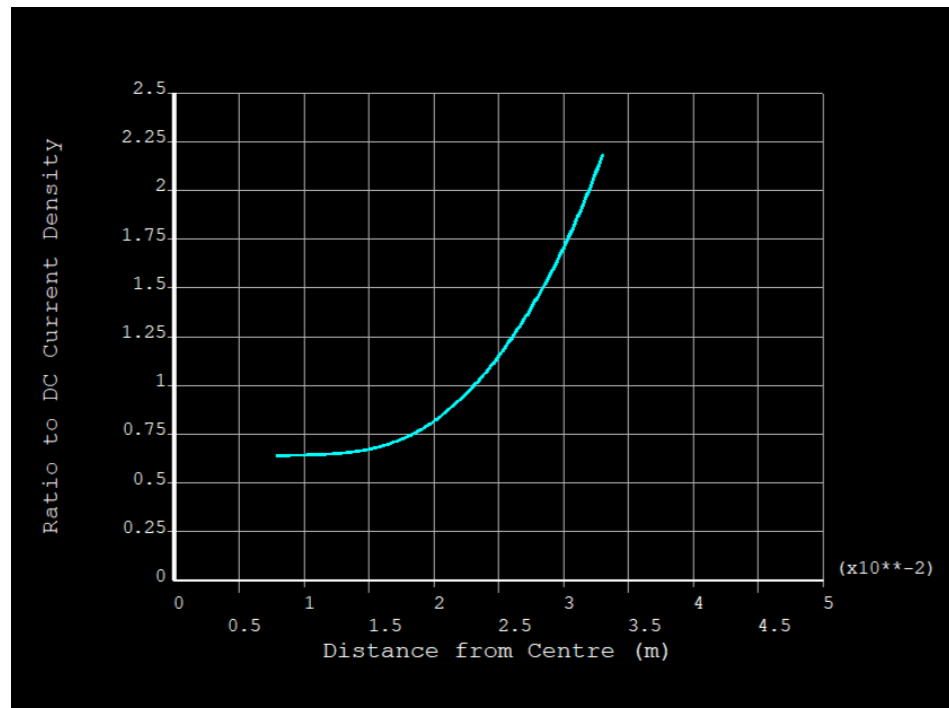### 5.5.2. Normalized Current Density Line Charts

Figure 10a–c present the normalized current density profiles for the 2D models. The normalized current density (J/J_{DC}) is calculated as the ratio of the local current density (J) to the uniform current density under DC conditions (J_{DC}). Here, J_{DC} represents the current density when the current is evenly distributed across the conductor's cross-sectional area, as is typical in direct current scenarios. These profiles illustrate how the current density varies across the conductor's radius under alternating current conditions. As the number of segments increases, the current distribution becomes more uniform across the conductor's cross-section. The single-segment model shows a pronounced peak in current density near the conductor's surface, reflecting the strong influence of the skin effect. In the three-segment model, the current distribution is more balanced, with a noticeable reduction in peak concentrations. The five-segment model, while exhibiting improved uniformity, displays a slight increase in peak current density at the segment edges, likely due to geometric factors such as sharp edges that alter the local field distribution.

(**a**)

(**b**)

(**c**)

Figure 10. Normalized current density vs. distance from center at 50 Hz (2D models) of 1-segment (**a**), 3-segment (**b**) and 5-segment (**c**).
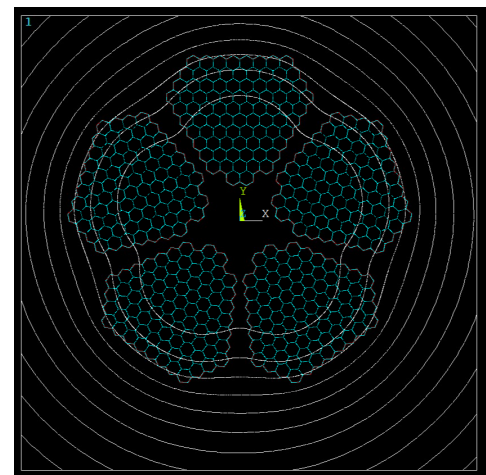
5.6. Magnetic Field Distribution Analysis

Magnetic flux density is a direct indicator of the electromagnetic fields generated by current flow within conductors. Figure 11a–c illustrate the magnetic flux line distributions for single-segment, three-segment, and five-segment 2D models at 50 Hz, respectively.
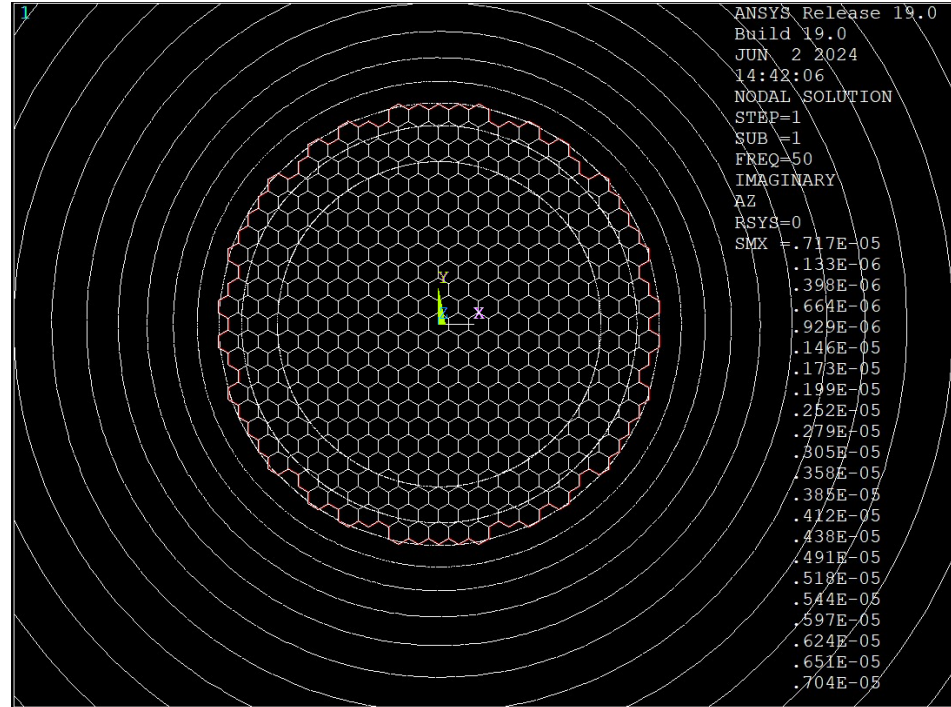
(**a**)
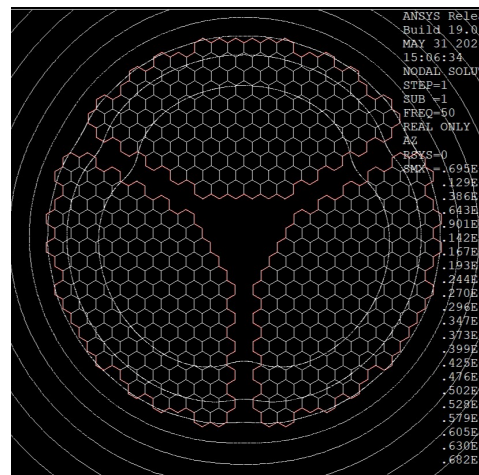
(**b**)

(**c**)

Figure 11. Magnetic flux line representation at 50 Hz for 1-segment (**a**), 3-segment (**b**) and 5-segment (**c**) 2D models.

The magnetic flux distributions indicate that in single-segment models, flux lines are densely concentrated near the conductor's boundaries, reflecting high magnetic flux density due to pronounced skin effects. As segmentation increases, the flux lines become more dispersed, indicating a reduction in localized magnetic field intensities. The five-segment model showcases a more uniform flux distribution, corroborating the effectiveness of segmentation in mitigating skin and proximity effects.

5.7. Computational Efficiency Analysis

Evaluating the computational efficiency of 2D versus 3D finite element (FE) models is essential for their practical application in engineering. This analysis compares the processing time and memory usage required to simulate single-segment, three-segment, and five-segment cable configurations using both 2D and 3D models, referencing the hardware specifications from Section 4.

5.7.1. Effective Run Time and Memory Utilization

To standardize computational effort, an *Effective Run Time* (ERT) metric is introduced, calculated by multiplying CPU time by the number of parallel cores used. This allows direct comparison between 2D and 3D models despite different parallelization strategies.

5.7.2. Analysis of Computational Efficiency

Table 7 highlights the stark differences in computational resources between 2D and 3D models:

- **Processing Time and Memory Usage**:
  - **2D Models**: Exhibit low ERT (2.8 to 3.6 h·c) and minimal RAM usage (6.7 to 8.2 GB), regardless of segmentation;
  - **3D Models**: Require significantly higher ERT (72.0 to 160.0 h·c) and memory (154.1 to 1072.4 GB), especially with increased segmentation and model length;

- **Segmentation Impact**:
  - The five-segment 3D model demands the highest computational resources due to its complexity and length (4 m), whereas 2D models maintain consistent efficiency across segmentations.

Table 7. Computational resource utilization.

Segment	Parallel Cores	CPU Time (Hours)	ERT (h·c)	RAM Usage (GB)
1 Segment (2D)	4	0.7	2.8	6.7
3 Segment (2D)	4	0.9	3.6	7.1
5 Segment (2D)	4	0.9	3.6	8.2
1 Segment (3D)	24	3.1	74.4	154.1
3 Segment (3D)	24	3.0	72.0	373.2
5 Segment (3D)	64	2.5	160.0	1072.4

5.7.3. Comparative Efficiency

The comparison underscores the advantages of 2D models:

- **2D Models**:
  - Highly efficient with low ERT and RAM usage;
  - Performance remains stable across different segmentations, making them ideal for rapid and large-scale simulations;

- **3D Models**:
  - Substantially higher computational demands, limiting their practicality for extensive or iterative studies;
  - The complexity increases sharply with segmentation and length, posing significant challenges for simulating large-scale or twisted conductor configurations.

5.8. Mesh Refinement and Discretization Errors

Accurate FE simulations rely heavily on appropriate mesh density to minimize discretization errors. Table 4 summarizes the maximum discretization errors for different models, measured by the normalized flux density discrepancy (BN_{ERR}).

The 2D models exhibit lower discretization errors (0.19% to 0.30%) compared to the 3D models (1.72% to 2.39%). This disparity is primarily due to the larger model geometry in comparison with the element counts (which is limited by the computational resources) inherent in 3D simulations, which can introduce more numerical inaccuracies if not meticulously refined. Nevertheless, the overall low error percentages affirm the reliability of both modeling approaches for segmented cables with parallel conductors, with 2D models offering superior accuracy at reduced computational costs.

5.9. Validation of the FE Models

Ensuring the accuracy and reliability of FE simulations is paramount. The 3D models in this study were validated against established results from [12], which employed similar modeling techniques for multi-segment cable configurations at 50 Hz. The $R_{\text{AC}}/R_{\text{DC}}$ ratios from this study's 2D and 3D models closely align with the validated results, confirming the robustness of the Solver Machine framework implemented in ANSYS Mechanical APDL.

Table 8 presents a direct comparison of the $R_{\text{AC}}/R_{\text{DC}}$ ratios between this study and [12] as a benchmark for single-segment, three-segment, and five-segment models at 50 Hz. The $R_{\text{AC}}/R_{\text{DC}}$ ratios from both 2D and 3D models are in excellent agreement with the validated results from [12], with discrepancies well within acceptable engineering margins. This close alignment reinforces the credibility of the FE models and the Solver Machine framework used in this study, ensuring that the simulations accurately capture the electromagnetic behavior of segmented cables.

Table 8. Validation of $R_{\text{AC}}/R_{\text{DC}}$ ratios against [12].

Segment	Benchmark	2D Models	3D Models
1-Segment	1.86	1.85	1.86
3-Segment	1.76	1.76	1.76
5-Segment	1.73	1.74	1.75

6. Conclusions

This study compares two-dimensional (2D) and three-dimensional (3D) finite element (FE) models in analyzing skin and proximity effects in segmented power cables with parallel conductors. Evaluating single-, three-, and five-segment configurations across frequencies of 0, 50, 150, and 250 Hz, the research demonstrates that 2D models offer comparable accuracy to 3D models with significantly reduced computational resources.

The key findings of this study are as follows:

- **Accuracy of 2D Models**: Two-dimensional FE models achieved $R_{\text{AC}}/R_{\text{DC}}$ ratios within 2% of 3D models, with errors below 0.6% at 50 Hz. This validates their effectiveness in capturing electromagnetic behavior in parallel conductor conditions;
- **Computational Efficiency**: Two-dimensional models require substantially less processing time and memory, making two-dimensional models ideal for large-scale and iterative studies;
- **Impact of Segmentation**: Increasing segments from one to five slightly reduced the $R_{\text{AC}}/R_{\text{DC}}$ ratio, indicating mitigation of skin and proximity effects. However, the modest reduction suggests that additional strategies are needed to counteract skin effects at higher frequencies;

- **Frequency Dependence**: The R_{AC}/R_{DC} ratio increases with frequency, highlighting the need for design optimizations to manage skin effects in high-frequency applications. Segmentation provides partial mitigation but is insufficient alone;
- **Mesh Design Considerations**: Appropriate mesh density in 2D models is crucial for low discretization errors. While 3D models can achieve similar accuracy with fine meshes, their higher computational costs make 2D models more practical for many applications.

Despite these promising results, the study has limitations. Simulations focused only on the conductive core, assuming infinitely long cables with parallel flux lines and fully compressed hexagonal conductor arrangements. Additionally, materials were treated as homogeneous with fixed resistivity, ignoring potential variations from manufacturing processes or temperature changes.

Future research should incorporate additional cable components, explore finite-length effects and helical twisting, investigate non-parallel conductor arrangements. These advancements will enhance the robustness and applicability of FE models for diverse power cable designs.

In conclusion, 2D FE models are highly efficient and sufficiently accurate alternatives to 3D models for analysing skin and proximity effects in segmented cables with parallel conductors. The 2D and 3D FE simulations result in the same skin and proximity losses when all conductor strings are in parallel with each other. Future work will extend these models to include twisted or transposed conductors and advanced insulation layers, as well as material and temperature variations, to further investigate the skin and proximity effects in power cables. Integrating materials with μ_r greater than unit can potentially help in distributing flux lines more uniformly, which may result in lower skin and proximity losses.

References

1. Brauer, J.; Ochs, R. Skin effect and proximity effect in multiconductor systems with applied magnetic materials. *J. Appl. Phys.* **1991**, *69*, 5035–5037.
2. Gassab, O.; Chen, Y.; Shao, Y.; Li, J.; Wen, D.E.; He, F.; Su, Z.; Zhong, P.; Wang, J.; Zhao, D.; et al. Accurate Formulation of the Skin and Proximity Effects in High-Speed Cables. *IEEE Trans. Electromagn. Compat.* **2022**, *64*, 123–132. [CrossRef]
3. Patel, U.; Gustavsen, B.; Triverio, P. Fast computation of the series impedance of power cables with inclusion of skin and proximity effects. *IEEE Trans. Power Deliv.* **2013**, *28*, 2493–2501. [CrossRef]
4. da Silva, F.F.; Bak, C.L. Electromagnetic transients in power cables: A comprehensive review. *IEEE Electr. Insul. Mag.* **2013**, *29*, 15–24.
5. Ametani, A.; Ohno, T.; Nagaoka, N. *Cable System Transients: Theory, Modeling and Simulation*; Wiley-IEEE Press: Piscataway, NJ, USA, 2015.

6. Kuczmann, M.; Iványi, A. Modeling of Skin and Proximity Effects in Multi-Bundle Cable Lines. In Proceedings of the 2019 IEEE 13th International Symposium on Applied Computational Intelligence and Informatics (SACI), Timisoara, Romania, 29–31 May 2019; pp. 1–5.

7. Cavallini, A.; Montanari, G.C.; Hampton, R.N. Cable Parameter Variation Due to Skin and Proximity Effects: Determination by Means of Finite Element Analysis. In Proceedings of the 2009 IEEE Power & Energy Society General Meeting, Calgary, AL, Canada, 26–30 July 2009; pp. 1–8.

8. González-Teodoro, J.R.; Romero-Cadaval, E.; Asensi, R.; Kindl, V. Determination of Wire Resistance Caused by Skin Effect Using Modified 3D Finite Element Model. *Electr. Eng.* **2020**, *102*, 1513–1520. [CrossRef]

9. McAllister, D. *Electric Cables Handbook*; Grafton Books: Louisville, KY, USA, 1982.

10. Woodruff, L. *Principles of Electric Power Transmission and Distribution*; Wiley: New York, NY, USA, 1925.

11. Choi, J.H.; De Leon, F. Harmonic contributions of home appliances and their effects on power systems. *IEEE Trans. Power Deliv.* **2007**, *22*, 2548–2556.

12. Khan, S.; Grattan, K.T.V.; Attwood, J.R. Finite Element Modelling of Skin and Proximity Effects in High Voltage Power Cables. In Proceedings of the COMPUMAG, Evian, France, 2–5 July 2001; pp. 2–5.

13. Paice, D.A. *Power Electronic Converter Harmonics: Multipulse Methods for Clean Power*; IEEE Press: Piscataway, NJ, USA, 1981.

14. Gross, E. Proximity and Skin Effects in Conductors. *Proc. IRE* **1959**, *47*, 1524–1528.

15. Kraus, J.D. *Electromagnetics*, 4th ed.; McGraw-Hill: New York, NY, USA, 1991.

16. Goranovic, P.; Ostojic, G. Electrical Properties of Conductors and Cables. *IEEE Trans. Ind. Appl.* **2007**, *43*, 1403–1409.